Thermodynamic Evaluation of a Refrigeration Bottoming Cycle on the Efficiency of a Condensing Supercritical Carbon Dioxide Power Cycle

Phalgun N Malupillai
Graduate Researcher
University of Washington
Seattle, Washington

Jon D. McWhirter, PhD, P.E.
Sr. Manager MCFR, Thermal Hydraulics
TerraPower LLC,
Bellevue, Washington

Phalgun Malupillai is a Mechanical Engineering MS student at the University of Washington, currently working as a research intern with TerraPower. He holds a B.Tech in Chemical Engineering from NIT Trichy, and has a strong interest towards thermodynamics, clean energy, and carbon capture.

Jon McWhirter is Senior Manager, Molten Chloride Fast Reactor Thermal Hydraulics at TerraPower LLC in Bellevue, WA. He holds a Doctorate from The University of Texas at Austin, and Professional Engineer licenses in the states of Idaho and Washington.

Nomenclature

ΔT	Temperature Difference (˚C)	Q	Heat Duty (kJ)
COP	Coefficient of Performance	s	Specific Entropy (kJ/kg-K)
C_p	Specific Heat Capacity (kJ/kg-K)	sCO_2	Supercritical CO_2
HEX	Heat Exchanger	T	Temperature (˚C)
HTR	High Temperature Recuperator	T_o	Dead state Temperature (˚C)
i	Irreversibility (kJ) *or* (kJ/s)	T_{Rej}	Heat Rejection Temperature (˚C)
LTR	Low Temperature Recuperator	T-S	Temperature - Entropy
$\dot{m}$	Mass flow rate (kg/s)	η	Efficiency
MSR	Molten Salt Reactor	Φ	Availability / Exergy (kJ)

Abstract

Supercritical Carbon Dioxide (sCO_2) power cycles have recently garnered attention for use with high temperature Gen IV nuclear reactors such as Molten Salt Reactors (MSR) due to prospects for improved performance in high temperature regions, with the Recompression model being one of the most studied configurations where the heat rejection step occurs near the CO_2 critical point of 30.98˚C. An alternative well researched variant is the transcritical condensing CO_2 cycle which reduces irreversibility in heat rejection and shows higher efficiencies and specific work produced. The stable operation of an MSR benefits from maintaining steady operating points, heat transfer and approach temperature between the salt loop and the power cycle. Given the proximity of the critical point of CO_2 to ambient temperatures, and the variability of thermodynamic properties near this point, sCO_2 cycles are susceptible to unwelcome transients associated with ambient temperature fluctuations. Further, condensing cycles, despite showing promising performance, are limited to regions with consistent ambient temperatures which allow heat rejection below the critical temperature, year-round.

This study proposes a "Thermal Adapter" model, which uses a refrigeration bottoming cycle to maintain stable operating points in a condensing sCO_2 recompression cycle, while allowing condensation irrespective of ambient conditions, thereby addressing both these concerns. The isothermal heat rejection from the CO_2 (in contrast to a Brayton cycle) to refrigerant, and refrigerant to the environment mitigates some of the work lost through the operation of the refrigeration cycle. A thermodynamic and exergy analysis was conducted comparing the Thermal Adapter model to the standard recompression cycle at varying environmental temperatures. The results indicate that the Thermal Adapter successfully isolates the CO_2 cycle and nuclear operation from transient ambient conditions, exhibiting a greater specific work at all ambient temperatures, a higher net efficiency at T_{Rej} > 32˚C, and operational simplicity on comparison with the Reference model.

Introduction

Recent years have seen large investments and technological advancements made towards the launch of Gen IV nuclear reactors, as a step towards more efficient, and inherently safer nuclear power. These reactors generate heat at higher temperatures compared to most existing powerplants, with TerraPower's Molten Salt Reactor slated to operate near 650˚C, allowing for a higher Carnot efficiency in the coupled power cycle.

One such advanced power cycle poised towards high temperature application is the supercritical carbon dioxide (sCO_2) cycles which operates at high efficiencies with relatively compact and simple plant layouts, providing economic and operational benefits over competing supercritical steam cycles [1], and helium Brayton cycles [2]. The advantages of sCO_2 cycles stem from the low compressibility of CO_2 near the critical point, minimizing compression work, ability to internally recuperate heat, and the high density of CO_2 in the expansion process, allowing for smaller machinery, and higher energy density [3]. The low critical point of CO_2 at 31˚C and 7.38 MPa allow the cycle to reject heat near ambient conditions. The recompression cycle which operates entirely above the critical pressure is one of the most studied configurations [4]. The condensing transcritical recompression CO2 cycle has been well studied by [5] and involves condensation of a part of the CO2 stream, which is pumped from the liquid phase to supercritical pressure, resulting in a higher net power and efficiency [6]. Wright et al. have described how a slight reduction in heat rejection temperature can lead to significant efficiency gains [7]. The higher efficiency of the condensing cycle can be partially explained by the slightly lower heat rejection temperature implemented to facilitate condensation, resulting in a higher Carnot efficiency. The gain in the real cycle efficiency is greater than the increase in the Carnot efficiency associated with the wider temperature range. This observation is explained through the greater second law efficiency of the cycle arising from nearly isothermal heat rejection via condensation and thereby lower irreversibility.

The common concerns associated with the industrial implementation of sCO_2 cycles are the variations of the thermodynamic fluid properties in the vicinity of the critical point and the impact this may have on the overall power cycle. Unlike traditional steam cycles, CO_2 cycles reject heat near ambient conditions, and given the critical point of CO_2 is near the ambient temperature in most geographies, environmental temperature fluctuations may further disrupt the stable operation of a sCO_2 power cycle. The steady performance and operation of molten salt reactors is benefitted by a constant, and predictable heat transfer out of the salt loop and into the CO_2 cycle, hence such aforementioned disturbances in the CO_2 cycle as a result of transient ambient conditions are undesirable. The condensing sCO_2 cycle solves one facet of this problem, by rejecting heat from the cycle at temperatures significantly below the critical temperature. This process bypasses the critical point, and thereby any associated thermodynamic instability regions, while exhibiting appreciable gains in efficiency and specific work. Nonetheless, such cycles are limited geographically to regions where a sufficiently cold natural heat sink is available and are yet susceptible to variations in external temperatures.

This study proposes the use of a refrigerating bottoming loop as a “Thermal Adapter”, which couples with the heat rejection step of a condensing sCO_2 cycle. The Thermal Adapter will serve to maintain a constant interface temperature with the CO_2, thereby isolating the power cycle and nuclear operations from variations in external temperatures, while allowing for condensation of CO_2 irrespective to climatic conditions. A well-designed refrigeration loop will employ heat transfer between both the CO_2 cycle, and the environment through largely isothermal phase change processes, thereby minimizing irreversibilities, and reaping the benefits of a condensing cycle, which recoups some of the work lost through the introduction of an additional process. This study reports the thermodynamic and exergy analyses on the implementation of a Thermal Adapter and outlines the use cases wherein the use of such a configuration results in net efficiency and performance benefits.

Modelling

The thermodynamic modelling of the sCO_2 power cycle is carried out through the Aspen HYSYS modelling software, using the Peng-Robinson equation of state. The alternate equations of state considered were Lee-Kesler-Plocker and Redlich-Kwong-Soave. Peng-Robinson was selected due to the ease of computation, and accuracy near the critical point.

The accuracy of the Aspen HYSYS model was verified through the replication of the state points in the recompression cycle described by Wright et al. [7]. The model showed a variance of less than 1% in the prediction of efficiency and a variance of 3.6% in prediction of specific power.

Reference Model

The Reference model is based on the well-studied recompression Brayton cycle model and is modelled around the schematic described by Wright et al. [7], with some modifications as documented in Table 1.

The heat source is defined as an isothermal reservoir at 650°C. This analysis studies the effect of ambient temperature fluctuation on the sCO_2 power cycle, hence the heat rejection temperature is varied from 15°C – 45°C. The high pressure point is 20 MPa, and the low pressure point post expansion is set slightly above the critical pressure at 7.7 MPa, when the rejection temperature is above the critical temperature of CO_2.

For a fair comparison with the Thermal Adapter model, the reference model is designed to allow for condensation when the rejection temperature is sufficiently below the critical temperature (T_{Rej} < 30°C). This study does not directly refer to the ambient temperature as local conditions such as availability of running water, the humidity of air, etc. will affect the approach temperature between the power cycle fluid and ambient conditions, therefore the rejection temperature is used to denote the temperature of the working fluid post the heat rejection step. In the Reference model, T_{Rej} refers to CO_2 temperature exiting the rejection step. The turbine outlet pressure is dropped to the saturation pressure corresponding to the heat rejection temperature, allowing for condensation during the heat rejection step. Studies have shown that the low variation of density between the vapor and liquid phases of CO_2 allow for a compressor to function as a pump for liquid CO_2, albeit at lower efficiencies. This study credits the Reference model with the ability to pump condensed CO_2 by means of a compressor, with no penalty on adiabatic efficiency.

Thermal Adapter Model

The previously defined reference model has been modified to include a simple propane refrigeration cycle which facilitates the condensation of the CO_2 in the CO_2 heat rejection step. The closed propane loop consists of a compressor, compressing the propane to the saturation pressure at ambient conditions. The propane vapor rejects heat to the environment, condensing into a saturated liquid, which is throttled to form a two-phase mixture. The throttle outlet pressure is based on the level of Joule-Thompson throttling required to drop the temperature to 12°C. The propane evaporates in the CO_2-Propane phase change heat exchanger consequently condensing CO_2 at 15°C. The low temperature range of the propane cycle (12°C to T_{Rej}), results in a high COP cycle. T_{Rej} in this model refers to the temperature of propane leaving the condenser. The propane cycle effectively isolates the CO_2 loop from any fluctuations in the ambient temperature through modifications in the mass flow rate, and pressure ratio to maintain a constant CO_2-propane interface temperature. Figure 1 displays a process flow diagram highlighting the thermodynamics state points for a T_{Rej} = 40°C case. The theoretical total efficiency of such a combined cycle can be calculated as follows.

$$\eta_{Overall} = \eta_{Top} - \frac{\left(1 - \eta_{Top}\right)}{COP}$$

The Thermal Adapter leverages the CO_2 condensation to replace the main compressor with a centrifugal pump. The condensation of CO_2 allows the turbine to operate at a higher pressure ratio, expanding the fluid to the expected saturation pressure at 15°C, well below the critical pressure to which traditional cycles are limited. Further, the constant heat rejection temperature of 15°C allows for finetuning of the split flow ratio to allow for more effective heat transfer in the low temperature recuperator.

<u>Split Flow Ratio</u>

The split flow ratio is defined as the amount of flow directed to the heat rejection step, and consequently the pump and LTR, as opposed to the re-compressor. This ratio is dictated by the heat transfer in the LTR. The hot side carries the low-pressure vapor CO_2, while the cold side carries the high-pressure liquid CO_2 which undergoes evaporation and superheating in the LTR. The difference in thermodynamic conditions results in a high difference in the specific heat capacity between the streams potentially leading to unfavorable heat transfer [8]. To allow for a constant approach temperature across the heat exchanger, the total heat capacity of both flows must be matched.

$$\dot{m}_h * Cp_h * \Delta T_h = \dot{m}_c * Cp_c * \Delta T_c$$

$$For\ constant\ approach\text{:}\ \Delta T_h = \Delta T_c\ ;\ (\dot{m}_h * Cp_h - \dot{m}_c * Cp_c) \rightarrow 0$$

Given the specific heat capacity is fixed by the pressure ratios, the mass flow is then controlled through the split flow ratio to optimize operation. Figure 2 displays the effect of split flow ratio on the difference in mass capacities ($\dot{m}_h C_{p,h} - \dot{m}_c C_{p,c}$) across the heat exchanger and the corresponding impact on overall cycle efficiency. The peak cycle efficiency is found at a split flow ratio of 0.544.

Results and Discussion

The performance of the Thermal Adapter Model and the Reference model are evaluated and compared under varying ambient temperature conditions (heat rejection temperature varies from 15°C to 45°C). The effect of the propane refrigeration loop on overall system performance, and the ability to isolate the power cycle from extraneous thermal fluctuations is documented in this section. The primary parameters of concern are system efficiency, specific work, and CO_2 inlet temperature to the primary salt heater.

<u>Efficiency</u>

Figure 3 shows that the thermal adapter model exhibits a significantly higher efficiency at all rejection temperatures above the critical point (T_{Rej} > 33°C). At points greater than the critical temperature, the Thermal Adapter model leverages isothermal phase change process to transfer heat from both the CO_2 into the propane loop and reject heat from the propane loop to the environment. This results in minimal heat transfer related entropy gain, and consequently high efficiencies.

At rejection temperatures below the critical temperatures, the theoretical reference model reaps the benefits of a condensing transcritical CO_2 cycle, without the parasitic load of the propane refrigeration cycle, resulting in a theoretical higher efficiency. However, to reject heat via condensation, the system must operate at higher pressure ratios, and repurpose the compressor to pump liquid CO_2. Studies have shown that such an application of compressors is possible, albeit at a less than ideal efficiency point thereby diminishing the overall cycle efficiency [9]. For the reference model to outperform the thermal adapter model while condensing CO_2 (T_{Rej} <31˚C), a compressor designed for an 85% peak efficiency for vapor phase application, must exhibit an adiabatic efficiency of greater than 75% while pressurizing the liquid phase. A more feasible operational strategy under colder ambient conditions ($T_{ambient}$ < 31°C) in a standard sCO_2 cycle would be to restrict the cooling of low-pressure CO_2 to near the critical temperature, consequently underleveraging the available natural heatsink, given the restrictions imposed by the turbomachinery. The operation of the Thermal Adapter model is not restricted by the ambient temperatures to the same degree, however, is still susceptible to efficiency losses arising from off-design operation of the Propane compressor.

Specific Work

Figure 4 depicts the variation of specific work produced by the cycle, with variations in the heat rejection temperature. The improved performance of the thermal adapter model is attributed to the higher-pressure ratio across the turbine, and the lower work required to pump liquid CO_2. The adapter model exhibits a 15% higher net work at T_{Rej} of 26°C, quickly rising to a 60% higher net work at a T_{Rej} of 39°C when compared to the reference model.

Impact on Salt Heat Exchange Process

The primary heat input step in the proposed nuclear power application is through a salt heat exchanger. The stable operation of the nuclear process benefits from maintaining a steady heat transfer between the salt and the attached power cycle. Figure 5 and Figure 6 depict the impact of variations in environmental conditions on the entry temperatures of CO_2 into the salt heat exchanger, as well as the heat absorbed by the power cycle for a 1 kg/s mass flow rate of CO_2, respectively. The graphs clearly show that the propane refrigeration loop successfully isolates the power cycle, and consequently the nuclear process from any transient environmental conditions, providing a constant CO_2 inlet temperature to, and constant Q_{out} from the salt loop.

T-S Diagram at T_{Rej} = 40°C

A comparison between the T-S diagrams of the Thermal Adapter model, and the Reference model, when operating under identical temperature boundary conditions is depicted in Figure 7 and Figure 8. This chart depicts the ability of the propane refrigeration loop to pull the CO_2 into the liquid phase, allowing for near isothermal heat rejection, as opposed to the large temperature gradient across the rejection step in the reference model. The ability of the propane loop to exchange heat isothermally with both the CO_2 loop, and the environment, results in an overall more efficient system. This behavior is consistent in all cases where T_{Rej} > 32˚C.

Exergy Analysis and Second Law Efficiency

A detailed exergy analysis was conducted to thermodynamically analyze and compare the performance of the Thermal Adapter model with the Reference model. The analysis assumes heat input through an isothermal heat source at 650°C, and an isothermal heat sink at the rejection temperature. The exergy entering the system, and the irreversibility of each of the unit processes are calculated based on the formulae in Table 2.

Figure 9 and Figure 10 display the comparison of irreversibility as a percentage of exergy entering the system for a 40°C heat rejection case. The irreversibility of the "Rejection" process in the Reference model refers solely to the work lost while rejecting heat to the environment. The irreversibility of rejection in the Thermal Adapter model refers to the sum of the work lost across the CO_2-propane heat exchanger, along with the work lost in the propane cycle (compressor, condenser, and throttle).

The data shows that the irreversibility of heat rejection is significantly lower in the Thermal Adapter model, despite the presence of additional equipment and processes. The facilitation of isothermal heat rejection from the CO_2 loop to the Propane loop as opposed to direct heat rejection to the atmosphere results in an overall less irreversible (more efficient) system. This behavior is exhibited for all cases where the heat rejection temperature is greater than the critical temperature of CO_2.

Conclusion

The benefits of a condensing transcritical CO_2 power cycles are well established in literature. A primary barrier associated with such a process is the proximity of the critical temperature to ambient conditions, wherein variations in environmental temperatures disrupt the ability to condense CO_2 in the heat rejection step. Further, this study is directed towards the application of sCO_2 cycles in the nuclear industry, where maintaining stable operating conditions in the power cycle and the nuclear plant, irrespective of transient ambient conditions, are of importance. This analysis follows a thorough modelling effort resulting in the development of a "Thermal Adapter" system which incorporates a propane refrigeration bottoming loop for a condensing CO_2 cycle and evaluates the ability of a such a loop to isolate the power cycle from ambient temperature fluctuations, and the effect of the bottoming loop on the thermodynamic performance of the overall system. The proposed system is compared against a standard condensing sCO_2 power cycle rejecting heat directly to the environment.

A thermodynamic and exergy analysis resulted in the following conclusions:

- The Thermal adapter model successfully isolates the power cycle from ambient thermal fluctuations, as measured by the constant inlet temperature to, and heat duty absorbed from the salt HEX. In contrast, a 25℃ variation in ambient temperature in the reference model results in an 83℃ variation in CO_2 inlet temp to the salt HEX.

- The Thermal Adapter model boasts of a higher specific work at almost all ambient temperatures, despite the presence of additional rotating equipment (12% higher at a T_{Rej} of 25℃, and 61% higher at 40˚C). This is attributed to a higher pressure ratio across the turbine, and ease of pressurizing liquid CO_2 as opposed to a gas compression process.

- The Thermal Adapter model exhibits a significantly higher efficiency than the reference model at all $T_{Rej} > 32$˚C, due to the isothermal heat rejection via condensation. The exergy analysis around this process shows that this isothermal rejection step compensates for the irreversibilities added by the propane loop, resulting in a net efficiency gain when compared to the Reference model.

The reference model in this study shows a higher efficiency when the T_{Rej} is between 25˚C and 32˚C, as the model benefits from the condensation of the CO_2 without the parasitic load of the refrigeration cycle. However, this performance is contingent on the compressor pressurizing liquid CO_2 at the same efficiency as gaseous CO_2, and such high performance has been shown to be unlikely. Further, the thermal adapter model may be modified such that when the ambient conditions are sufficiently low, the propane loop may be shut down, and the CO_2 stream can be redirected to reject heat directly to the environment, allowing for natural condensation. Following these two considerations, the authors believe that the Thermal Adapter model may thermodynamically outperform the reference model at all environmental conditions; however, further investigation is recommended. Additional perks of the newly devised set up are the ability to design a singular power cycle for application in various climatic zones with minor modifications to the refrigeration loop alone, which result in engineering design cost saving and commonality of hardware.

References

[1] Y. Ahn *et al.*, "Review of supercritical CO2 power cycle technology and current status of research and development," *Nuclear Engineering and Technology*, vol. 47, no. 6, pp. 647–661, Oct. 2015, doi: 10.1016/J.NET.2015.06.009.

[2] V. Dostal, P. Hejzlar, and M. J. Driscoll, "The Supercritical Carbon Dioxide Power Cycle: Comparison to Other Advanced Power Cycles," *Nucl Technol*, vol. 154, no. 3, pp. 283–301, Jun. 2006, doi: 10.13182/NT06-A3734.

[3] S. M. Besarati and D. Y. Goswami, "Supercritical CO2 and other advanced power cycles for concentrating solar thermal (CST) systems," *Advances in Concentrating Solar Thermal Research and Technology*, pp. 157–178, Jan. 2017, doi: 10.1016/B978-0-08-100516-3.00008-3.

[4] E. G. Feher, "The supercritical thermodynamic power cycle," *Energy Conversion*, vol. 8, no. 2, pp. 85–90, Sep. 1968, doi: 10.1016/0013-7480(68)90105-8.

[5] G. Angelino, "Carbon dioxide condensation cycles for power production," *J Eng Gas Turbine Power*, vol. 90, no. 3, pp. 287–295, 1968, doi: 10.1115/1.3609190.

[6] Y. M. Kim, C. G. Kim, and D. Favrat, "Transcritical or supercritical CO2 cycles using both low- and high-temperature heat sources," *Energy*, vol. 43, no. 1, pp. 402–415, 2012, doi: https://doi.org/10.1016/j.energy.2012.03.076.

[7] S. A. Wright, R. F. Radel, T. M. Conboy, and G. E. Rochau. (2011). Modeling and experimental results for condensing supercritical CO2 power cycles, doi: 10.2172/1030354.

[8] J. Sarkar and S. Bhattacharyya, "Optimization of recompression S-CO2 power cycle with reheating," *Energy Convers Manag*, vol. 50, no. 8, pp. 1939–1945, Aug. 2009, doi: 10.1016/J.ENCONMAN.2009.04.015.

[9] S. A. Wright, R. F. Radel, M. E. Vernon, P. S. Pickard, and G. E. Rochau. (2010). "Operation and analysis of a supercritical CO2 Brayton cycle.". doi: 10.2172/984129.

Tables

Parameters	Reference Model	Thermal Adapter Model
High Pressure	20 MPa	20 MPa
T_{Source}	650°C	650°C
HTR Approach Temp	4°C	4°C
LTR Approach Temp	3.5°C	3.5°C
Total Mass Flow	1 Kg/s	1 Kg/s
Split Ratio (To Heat Rejection)	0.604	0.544
$T_{Rejection}$ (T_{Rej})	15°C – 45°C	15°C – 45°C
$\eta_{\text{Main-compressor}}$	0.85	-
η_{Pump}	-	0.85
$\eta_{\text{Re-compressor}}$	0.87	0.87
η_{Turbine}	0.9	0.9
$\eta_{\text{Propane Compressor}}$	-	0.9
CO_2-Propane HEX Approach Temp	-	3°C
CO_2 Condensation Temp	-	15°C
Pressure Drop	5% of total	5% of total

Table 1: Model Parameters

278

Component	**Formula**
Exergy flow in	$\Phi_{in} = Q_{in} * (1 - \frac{T_o}{T_{source}})$
Turbomachinery	$i_{Turbo} = \dot{m} * T_o * (s_{out} - s_{in})$
Valve	$i_{valve} = \dot{m} * T_o * (s_{out} - s_{in})$
Heat Exchanger	$i_{HEX} = T_o * [\dot{m}_h(s_{h,out} - s_{h,in}) + \dot{m}_c(s_{c,out} - s_{c,in})]$
Heater	$i_{heater} = T_o * [\dot{m} * (s_{out} - s_{in}) - \frac{Q_{in}}{T_{source}}]$
Cooler	$i_{cooler} = T_o * [\dot{m} * (s_{out} - s_{in}) + \frac{Q_{out}}{T_{sink}}]$

Table 2: Exergy Analysis Calculations

Figures

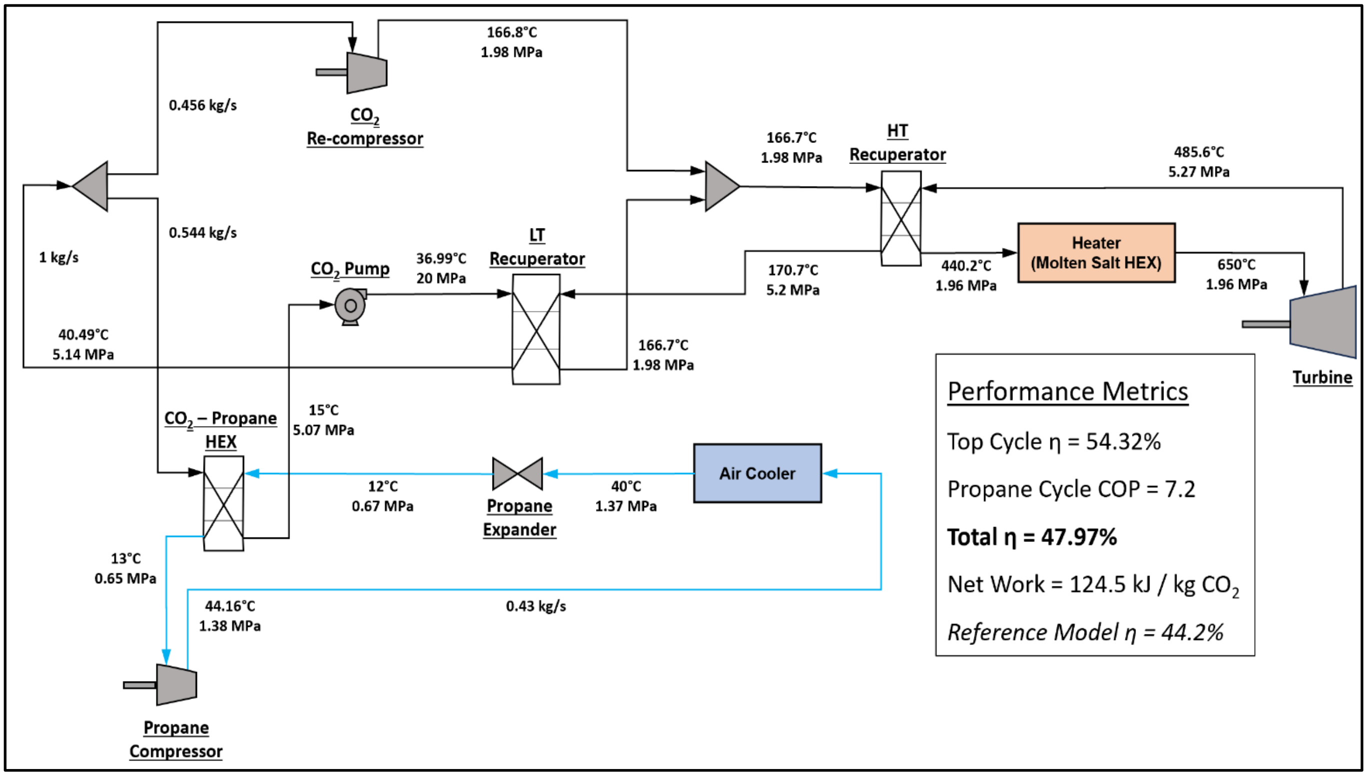

Figure 1: Model Schematic (T_{Rej} = 40 C)

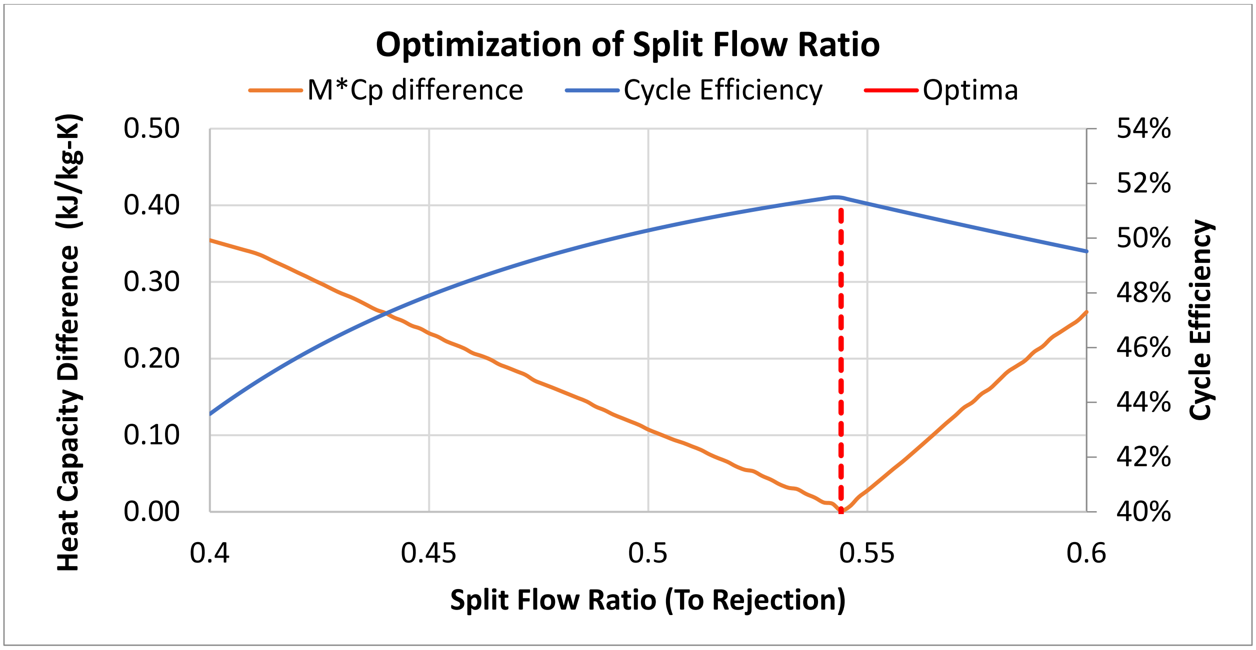

Figure 2: Split Flow Ratio Optimization

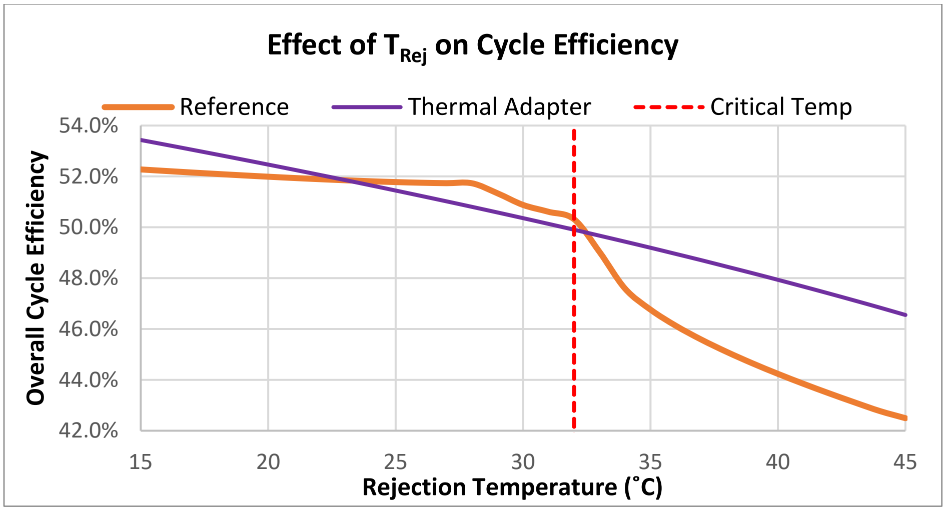

Figure 3: Efficiency v/s T_{Rej}

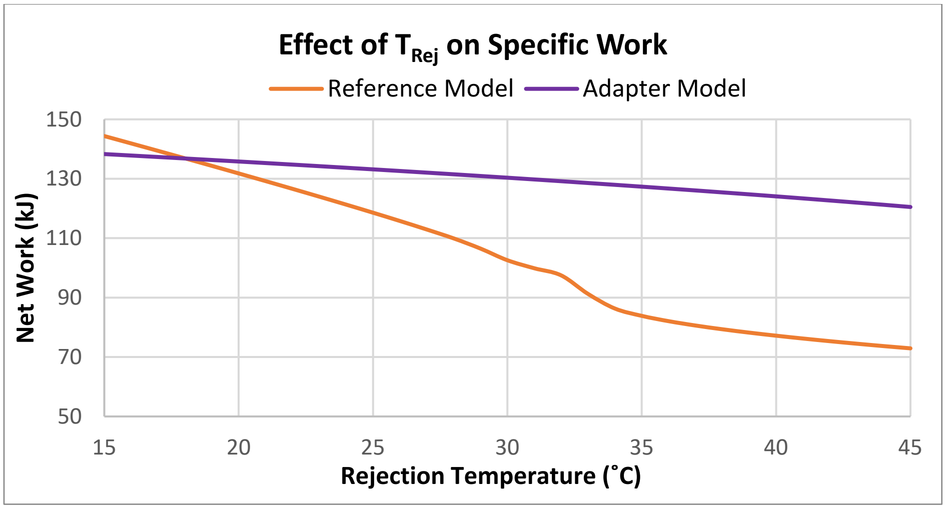

Figure 4: Specific Work v/s T_{Rej}

298

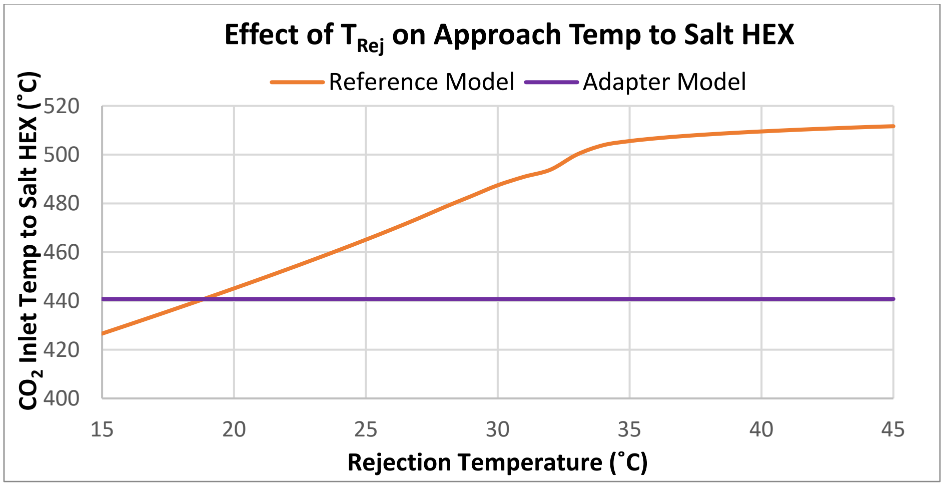

299

300 *Figure 5: CO_2 Approach temp to Salt HEX v/s T_{Rej}*

301

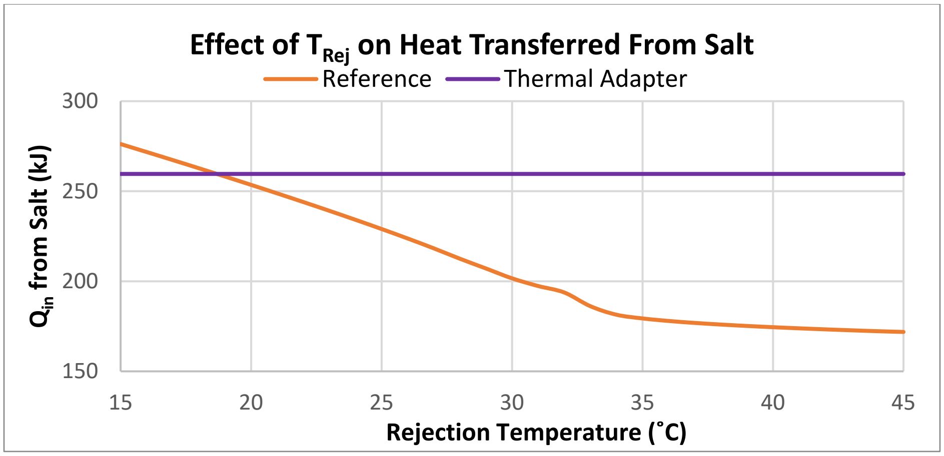

Figure 6: Heat duty absorbed from Salt v/s T_{Rej}

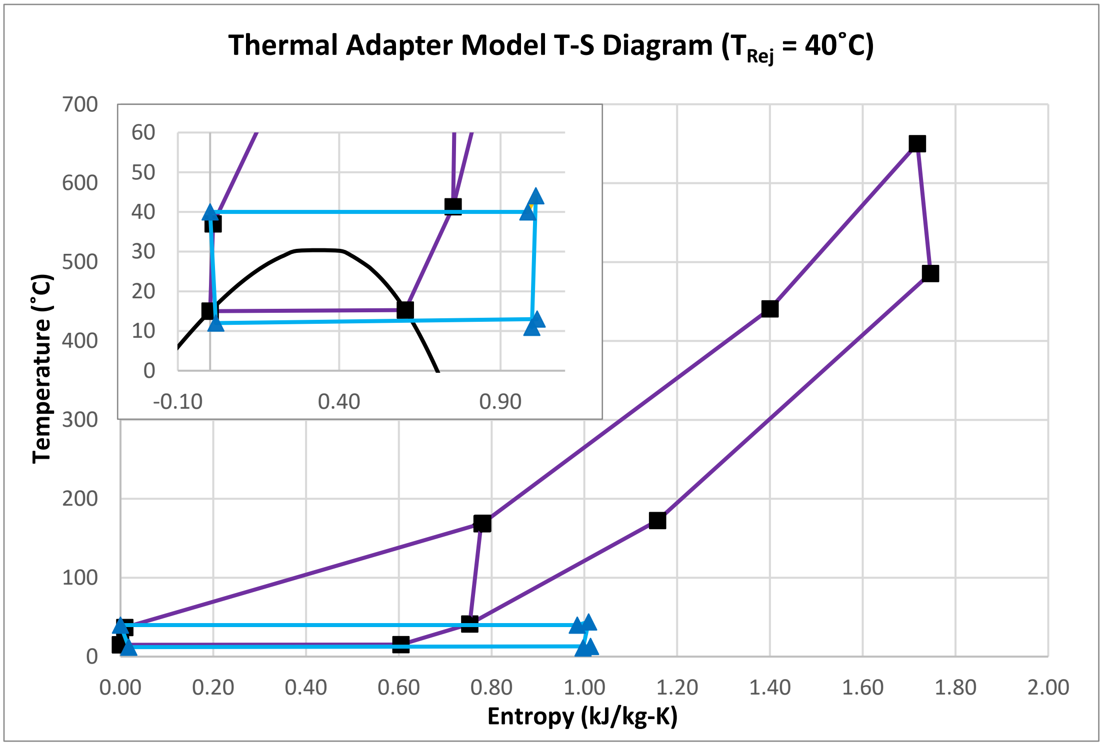

Figure 7: T-S Diagram of Thermal Adapter Model

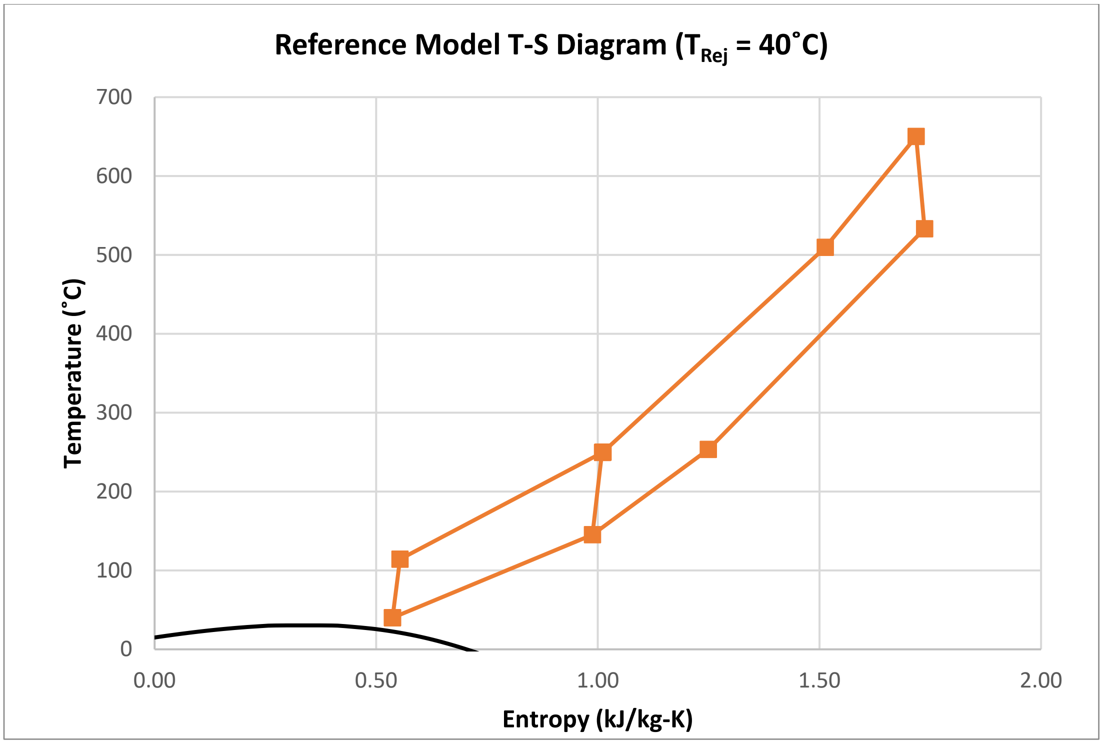

Figure 8: T-S Diagram of Reference Model

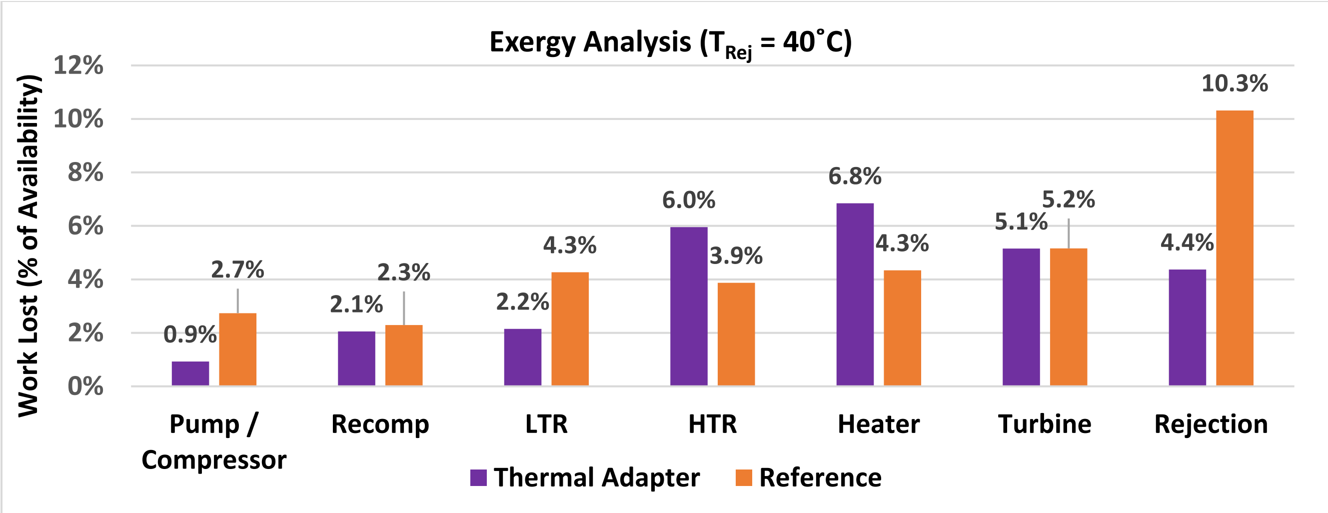

Figure 9: Exergy Analysis Results

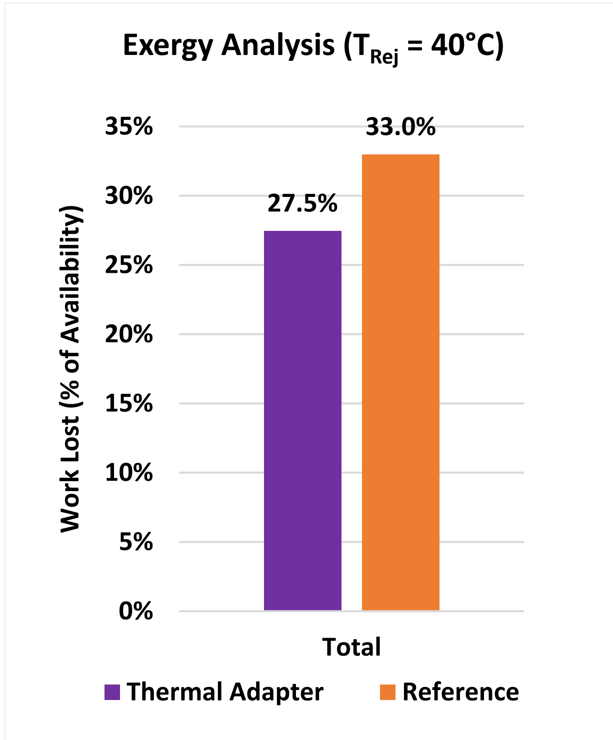

Figure 10: Exergy Analysis Results (Total)

Appendix A

Analysis of Ideal and Real Heat Engine – Refrigerator Combined Cycle

Jon D. McWhirter, Ph.D., P.E.

TerraPower, LLC

1 PURPOSE

This work is to demonstrate the thermodynamic feasibility of a combined cycle with sub-ambient heat rejection from a power cycle to a refrigeration system then ultimate heat rejection above the ambient temperature.

2 NOMENCLATURE

η - efficiency
T - temperature
Q - heat
β - coefficient of performance of refrigerator
W - work

3 SUMMARY

The Supercritical CO_2 Brayton cycle with Recuperation and Recompression, being investigated by various parties for application to nuclear plants but may suffer from issues related to the instability of operations in the vicinity of the critical point. The ambient temperatures worldwide vary enough to be above and below the CO_2 critical point of 31.1 °C. A combined cycle with Supercritical CO_2 power cycle rejecting heat to a refrigeration cycle is a potential scheme to maintain stable operating points of the CO_2 while having the 'bottoming' refrigeration cycle as a 'thermal adapter' to absorb variations in the ambient temperature while maintaining fixed CO_2 state points. To demonstrate that there is no violation of the Second Law of Thermodynamics, it is shown that the overall cycle efficiency does not exceed the Carnot Cycle efficiency for a heat engine operating between a high temperature reservoir and the ambient temperature. It is emphasized that the combined cycle efficiency is not guaranteed to be higher that the stand-alone Brayton cycle.

4 BACKGROUND

The Supercritical CO_2 Brayton cycle with Recuperation and Recompression is being investigated by various parties for application to nuclear plants (Dostal, Driscoll, & Hejzlar, 2004). However, the potential difficulty of maintaining stability in the vicinity of the critical point, 31.1 °C, and the strong variation of the cycle performance as the ambient temperature changes, are complications, though some analyses show stable operation of a compressor in the vicinity of the critical point (Wright, Radel, Vernon, Rochau, & Pickard, 2010). The notion of using a refrigeration cycle to create a stable *cold space* for the power cycle heat to be rejected to is proposed as a method of avoiding the issues associated with the critical point and the ambient temperature variation by having the heat sink sufficiently cool so that the CO_2 can be readily condensed regardless of the ambient temperature. To demonstrate that there is no violation of the Second Law of Thermodynamics, ideal efficiencies (i.e., Carnot) for the heat engine and the refrigerator are employed to arrive at equations demonstrating the efficiency for such a scheme relative to the Carnot efficiency.

5 ANALYSIS

5.1 Combined cycle description

A schematic of the system is shown below in Figure 1. Four thermal reservoirs are involved: the high temperature Heat Source at T_H, the ultimate Heat Sink at $T_{AMBIENT}$, the heat rejection temperature for the heat engine T_L, and the cold space temperature for the refrigerator, $T_{L'}$. For heat to flow from the heat engine heat sink temperature to the refrigerator cold space, a temperature difference, $DT = T_L - T_{L'} \geq 0$, is introduced. Heat from a high temperature reservoir is converted to work in a Carnot cycle with the rejected heat discharged to heat engine heat sink; this heat in its entirety then flows to a colder temperature region generated by the refrigeration cycle. The Carnot refrigerator then takes this quantity of heat, and with a portion of the work produced by the heat engine, compresses the refrigerant to a temperature at ambient; the ultimate heat rejected must include the contribution due to the refrigeration compressor work. The combined cycle net work, W_{NET} is then the heat engine work W_{HE} less the work required for the refrigeration compressor, W_{REF}.

5.2 Ideal Analysis

Beginning with a standard Carnot Heat Engine (Van Wylen & Sonntag, 1986) operating between a thermal reservoir heat source at T_H and a thermal reservoir heat sink at T_L, we have:

$$\eta_{CARNOT} = 1 - \frac{T_L}{T_H} \tag{7-1}$$

so

$$W_{HE} = Q_H \left(1 - \frac{T_L}{T_H}\right) \tag{7-2}$$

And, by reversibility and the definition of absolute temperature,

$$\frac{Q_H}{T_H} = \frac{Q_L}{T_L} \tag{7-3}$$

Thus

$$W_{HE} = Q_L \frac{T_H}{T_L}\left(1 - \frac{T_L}{T_H}\right) = Q_L \left(\frac{T_H}{T_L} - 1\right) \tag{7-4}$$

Next we introduce a Carnot Refrigerator absorbing heat at $T_{L'}$ and rejecting heat to the ambient at $T_{AMBIENT}$.

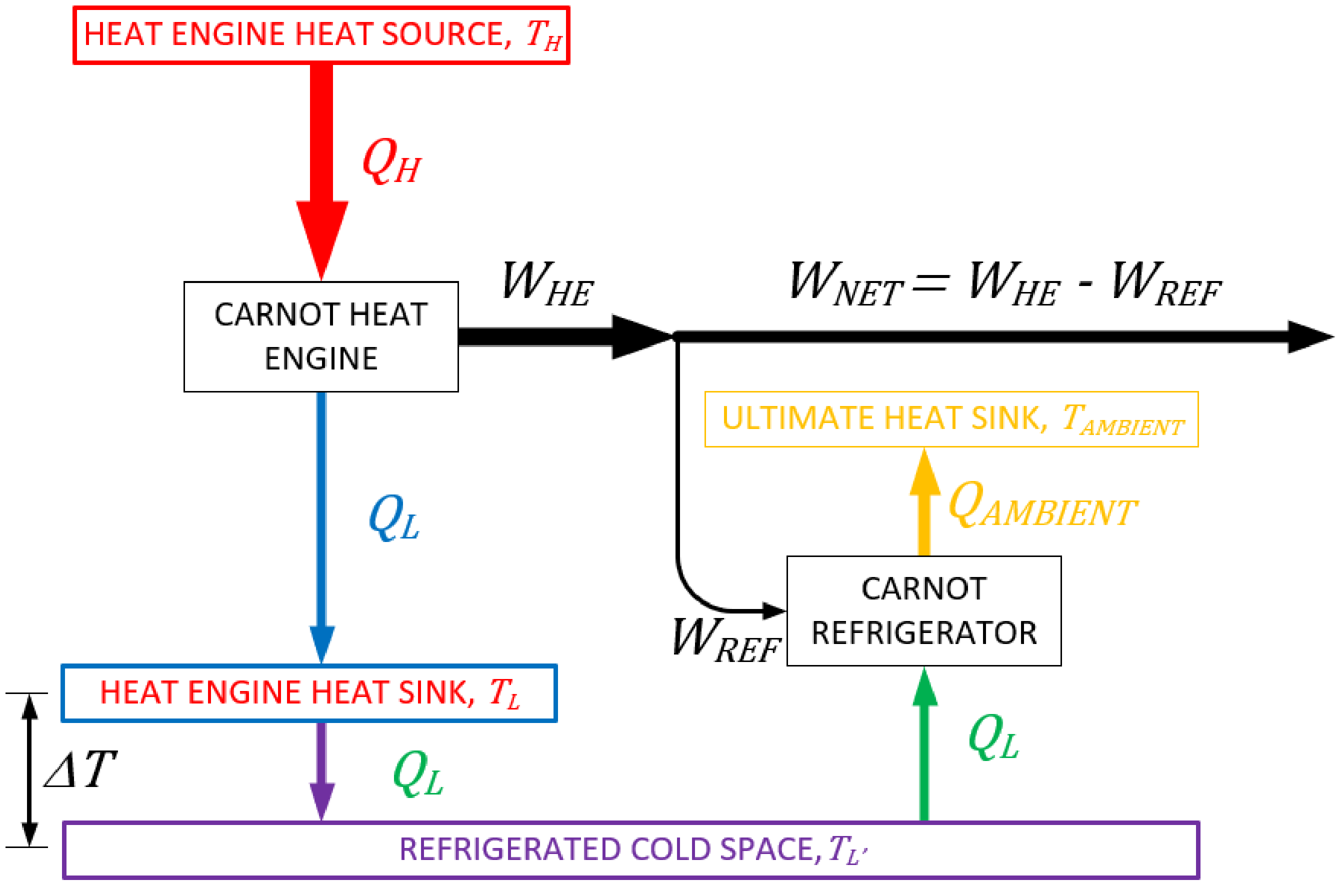

Figure 11: Schematic of the Combined Cycle

The Coefficient of Performance of the Carnot Refrigerator (Van Wylen & Sonntag, 1986) is

$$COP_{CARNOT} = \beta_{CARNOT} = \frac{Q_L}{W_{REF}} = \frac{Q_L}{Q_{AMBIENT} - Q_L} = \frac{T_{L'}}{T_{AMBIENT} - T_{L'}} \tag{7-5}$$

So

$$W_{REF} = Q_L\left(\frac{T_{AMBIENT} - T_{L'}}{T_{L'}}\right) = Q_L\left(\frac{T_{AMBIENT}}{T_{L'}} - 1\right) \tag{7-6}$$

Hence

$$W_{NET} = W_{HE} - W_{REF} = Q_L\left(\frac{T_H}{T_L} - 1\right) - Q_L\left(\frac{T_{AMBIENT}}{T_{L'}} - 1\right) \tag{7-7}$$

The goal is to find the overall efficiency, $h_{OVERALL}$, as a function of the thermal reservoir and ambient temperatures and the difference between the two low-temperature reservoirs, *DT*. Since

$$W_{NET} = W_{HE} - W_{REF} = Q_L\left\{\left(\frac{T_H}{T_L} - 1\right) - \left(\frac{T_{AMBIENT}}{T_{L'}} - 1\right)\right\} = Q_L\left\{\frac{T_H}{T_L} - \frac{T_{AMBIENT}}{T_{L'}}\right\} \tag{7-8}$$

$$W_{NET} = Q_H\frac{T_L}{T_H}\left\{\frac{T_H}{T_L} - \frac{T_{AMBIENT}}{T_{L'}}\right\} = Q_H\left\{1 - \frac{T_L}{T_H}\frac{T_{AMBIENT}}{T_{L'}}\right\}$$

$$\therefore \eta_{OVERALL} = \frac{W_{NET}}{Q_H} = \left\{1 - \frac{T_L}{T_H}\frac{T_{AMBIENT}}{T_{L'}}\right\}$$

With the <u>power cycle</u> heat rejection temperature slightly higher than the <u>refrigeration cycle</u> heat removal temperature,

$$T_L = T_{L'} + \Delta T, \Delta T > 0 \tag{7-9}$$

there results:

$$\eta_{OVERALL} = \frac{W_{NET}}{Q_H} = 1 - \left(\frac{T_{L'} + \Delta T}{T_H}\right)\left(\frac{T_{AMBIENT}}{T_{L'}}\right)$$

$$\therefore \eta_{OVERALL} = 1 - \left(\frac{T_{L'} + \Delta T}{T_{L'}}\right)\left(\frac{T_{AMBIENT}}{T_H}\right) \tag{7-10}$$

Now for some limiting cases. Note that for *DT* = 0, we arrive at the expected overall efficiency for an ideal heat engine operating between the high temperature reservoir and the ambient, η_{CARNOT}:

$$\Delta T = 0 \rightarrow \eta_{OVERALL} = 1 - \left(\frac{T_{L'}}{T_{L'}}\right)\left(\frac{T_{AMBIENT}}{T_H}\right) = 1 - \frac{T_{AMBIENT}}{T_H} = \eta_{CARNOT} \tag{7-11}$$

for a cycle between T_H and $T_{AMBIENT}$. Now, as *DT* > 0 (by definition), the overall efficiency is less than the Carnot efficiency – the numerator of the subtrahend in Eq. (7-11) is larger than that of the ideal case, so the difference is smaller. Hence, the Second Law of Thermodynamics remains observed since the Carnot cycle efficiency is not exceeded. Some other observations of the mathematics can be demonstrated more readily by looking at the ratio of the Carnot efficiency and the Overall Efficiency:

$$\frac{\eta_{OVERALL,\Delta T\neq 0}}{\eta_{CARNOT}} = \frac{1-\left(\frac{T_{L'}+\Delta T}{T_{L'}}\right)\left(\frac{T_{AMBIENT}}{T_H}\right)}{1-\frac{T_{AMBIENT}}{T_H}} = \frac{1-\left(\frac{T_{AMBIENT}}{T_H}\right)-\left(\frac{\Delta T}{T_{L'}}\right)\left(\frac{T_{AMBIENT}}{T_H}\right)}{1-\frac{T_{AMBIENT}}{T_H}}$$

$$\frac{\eta_{OVERALL,\Delta T\neq 0}}{\eta_{CARNOT}} = \frac{(T_H - T_{AMBIENT}) - T_{AMBIENT}\left(\frac{\Delta T}{T_{L'}}\right)}{(T_H - T_{AMBIENT})}$$

$$\therefore \frac{\eta_{OVERALL,\Delta T\neq 0}}{\eta_{CARNOT}} = 1 - \frac{T_{AMBIENT}\left(\frac{\Delta T}{T_{L'}}\right)}{T_H - T_{AMBIENT}} < 1, \forall\, \Delta T > 0 \qquad (7\text{-}12)$$

So as derived above, the Carnot efficiency is approached as $\Delta T \longrightarrow 0$. Also, the relative deviation from Carnot efficiency rises as $T_{AMBIENT}$ rises, a reasonable expectation.

6 REAL CYCLES

The objective of the real cycle analysis is to express the efficiency of an overall cycle in terms of the performance metrics of the heat engine and the refrigeration system. For a real heat engine with efficiency *h* and a refrigeration cycle with coefficient of performance b, with appropriate temperatures to foster the heat flows from higher to lower temperature, the work produced by the heat engine, for a heat input Q_H, is $W_{HE} = h\, Q_H$. The rejected heat is, therefore,

$$Q_L = (1-\eta)Q_H \qquad (7\text{-}13)$$

which is the heat that must be *lifted and rejected* by the refrigeration cycle. The coefficient of performance, β, for the refrigeration cycle is

$$\beta = Q_L/W_{REF} \Rightarrow Q_L = \beta W_{REF} \qquad (7\text{-}14)$$

substituting for Q_L yields

$$W_{REF} = (1-\eta)Q_H/\beta \qquad (7\text{-}15)$$

The net work for the system is the heat engine work less the refrigeration cycle work, or

$$W_{NET} = W_{HE} - W_{REF} = \eta Q_H - \frac{(1-\eta)Q_H}{\beta} = Q_H(\eta - (1-\eta)/\beta) \tag{7-16}$$

The overall efficiency is found by dividing the net work by the heat input, or

$$\eta_{OVERALL} = \eta - (1-\eta)/\beta \tag{7-17}$$

7 CONCLUSIONS

Ideal and real analyses have demonstrated that such a combined cycle with a *cold space* operating below ambient temperature, created by a refrigeration cycle rejecting heat to ambient, follows expected behavior mathematically. However, the test of whether this results in a gain over the 'original' Brayton cycle rejecting heat directly to ambient alone is not evaluated herein. That analysis is more complicated mathematically and must be realistically evaluated numerically with real thermodynamic state point data.

8 BIBLIOGRAPHY

Dostal, V., Driscoll, M., & Hejzlar, P. (2004). *A Supercritical Carbon Dioxide Cycle for Next Generation Nuclear Reactors.* Cambridge, Massachusetts : MIT.

Van Wylen, G., & Sonntag, E. (1986). *Fundamentals of Classical Thermodynamics, 3rd edition.* John Wiley & Sons.

Wright, S., Radel, R., Vernon, M., Rochau, G., & Pickard, P. (2010). *Operation and Analysis of a Supercritical CO2 Brayton Cycle, SAND2010-0171.* Sandia National Laboratory.